Polarized Emission and Optical Waveguide in Crystalline Perylene Diimide Microwires

By *Qiaoliang Bao, Bee Min Goh, Bin Yan, Ting Yu, Zexiang Shen,* and *Kian Ping Loh**

The use of organic nano/microstructures as interconnectors for the development of miniaturized optoelectronic devices has attracted a great deal of research interest. Recently, one-dimensional nano- and microstructures based on polymers[1,2] and small organic compounds[3–5] were demonstrated to be effective building blocks for light emission, routing, detection and modulation, similar to their inorganic counterparts.[6–8] For optoelectronic applications, fluorine-based π-conjugated organic compounds have many advantages such as high photoluminescence (PL) quantum efficiency, large stimulated emission cross-section, chemically tunable emission wavelength and abilities to form crystalline aggregate via self-assembly.[1–3] Perylene is a widely used dye molecule due to its high fluorescence quantum yield and chemical stability.[9] Perylene derivatives have long been studied as promising π-conjugated semiconductors for all organic photovoltaic solar cells[10] as well as n-type field effect transistors[11] due to its electron accepting and transporting ability. However, its applications in optoelectronics and waveguiding have not been reported.

To develop highly efficient waveguide based on organic wires, there are several basic requirements.[1–5] A large Stokes shift is needed to avoid re-absorption of propagating light. In addition, high purity and well-oriented crystals are important to ensure high PL efficiencies and less scattering from domain boundary. The wires must have uniform geometry and smooth surface to reduce scattering loss during light propagation. Although one-dimensional nanostructures of perylene and its derivatives, e.g., nanoneedles (diameter: ~80–400 nm, length: hundreds micrometers),[11] nanorods (diameter: ~50 nm, length < 1 μm),[12] nanobelts (width: ~200 nm, thickness: ~100 nm, length: tens of micrometers)[13,14] have been synthesized, highly efficient waveguide performance have not been obtained from these. In this work, we have prepared high-quality perylene diimide (PDI) microwires with uniform cylindrical shape and lengths of several hundred micrometers to millimeters, making them ideal candidates for low-loss ultralong optical waveguide and optoelectronic interconnectors. These high-quality PDI microwires were synthesized in a single phase solvent (dimethyl fluoride) using graphene oxide (GO) as the seeding agents, in contrast to the biphasic solvent methods (chloroform and methanol) used previously.[15] It appears that the template-assisted assembly of PDI on the surface of GO allows the growth of highly crystalline, smooth microwires that exhibit good optical properties.

Figure 1a shows representative dark-field optical image. The PDI microwires exhibit red emission. The bright PL spots at the tips and weak emission from the bodies clearly indicate that PL emission propagates along the wire axis, resulting in enhanced light emission at the tips where routed light exit the wire. This is the characteristics of active waveguide behavior. Long microwires (length > 200 μm) with apparent axial curvature can also show waveguide properties, as shown by the inset of Figure 1a. When the PDI microwire is excited with a green laser, the waveguide behavior is prominent and light coupling between multiple wires is also observed (see Figure S1 in the Supporting Information).

To achieve effective waveguiding, defects- and/or surface-induced scattering loss should be suppressed.[2,8] The microstructure and surface morphologies of as-synthesized microwires were examined using high-resolution bright-field transmission electron microscopy (TEM) and atomic force microscopy (AFM), the images are shown in Figure 1b and Figure S2. The images show that the PDI microwire fabricated in this work has regular and smooth surface with low density of defects, making them ideal as optical components.

The crystal structure was investigated by X-ray diffraction (XRD) (Figure 1c). The principal lattice planes are clearly resolved and can be used for the determination of lattice parameters based on the P1 space group: a = 4.69 Å, b = 8.57 Å, c = 20.02 Å, $\alpha = 86.28°$, $\beta = 90.16°$, $\gamma = 81.96°$. The PDI molecules exhibit slipped π-π stacking in the [100] direction (a-axis), as shown by the inset of Figure 1c. This is consistent with theoretical prediction as well as previous experimental reports that PDI-C8 crystal shape is elongated along the [100] direction.[11] The molecular stacking is well-known from other large perylene derivatives[16] and underscores the possibility of optical polarization discussed hereafter. Figure 1d displays the intensity-normalized UV absorption and PL spectra of PDI solution and microwires deposited on quartz. The solution absorption exhibits three resolved bands at 455, 485 and 521 nm, which correspond to vibronic 0–2, 0–1 and 0–0 transitions respectively.[13,14] The absorption spectrum of PDI microwires is considerably broadened and red-shifted, with fine vibronic structure in 500–600 nm range. The PL spectrum of PDI solution exhibits two peaks at 537 and 571 nm, corresponding to the 0–0 and 0–1 singlet exciton transitions of PDI. The long wavelength tail above ~600 nm is possibly due to fluorenone defect emission or unresolved vibronic replicas. In contrast, the

[*] Dr. Q. Bao, B. M. Goh, Prof. K. P. Loh
Department of Chemistry
National University of Singapore
3 Science Drive 3, Singapore 117543 (Singapore)
E-mail: chmlohkp@nus.edu.sg
B. Yan, Prof. T. Yu, Prof. Z. X. Shen
Division of Physics and Applied Physics
School of Physical and Mathematical Sciences
Nanyang Technological University
Singapore 637371 (Singapore)

DOI: 10.1002/adma.201000731

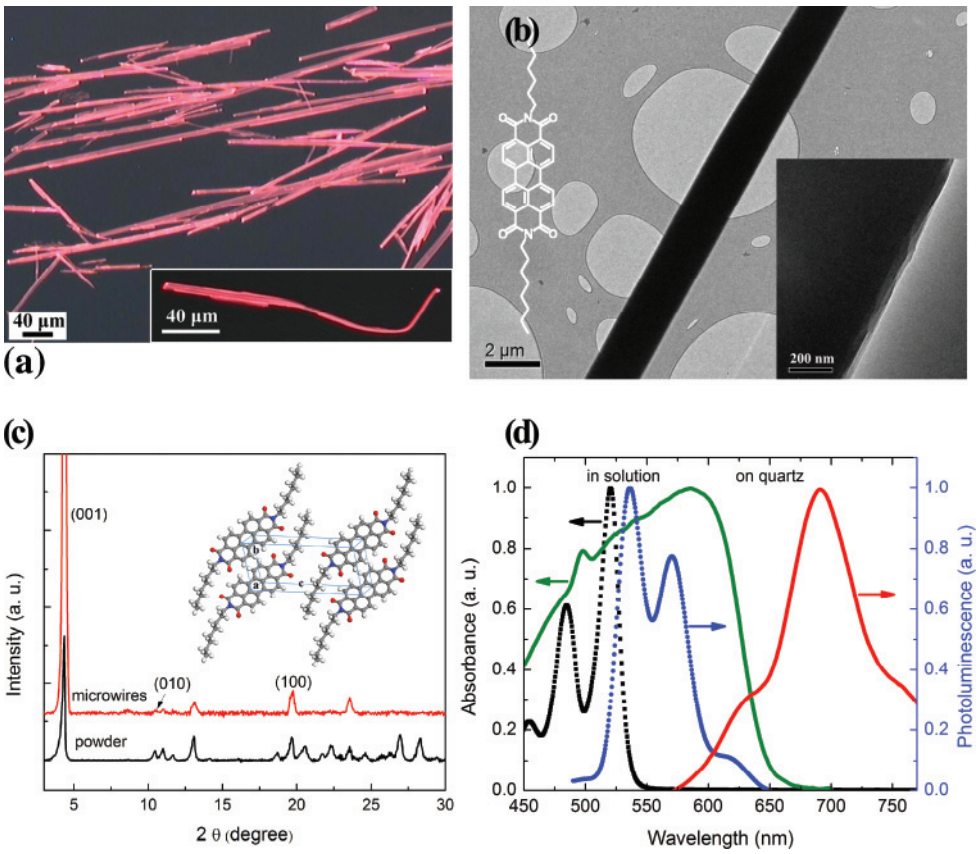

Figure 1. a) Dark-field image of PDI wires on a glass substrate. Inset shows a curved wire. b) Bright-field TEM image of a PDI wire. Inset: chemical structure of PDI and higher magnification TEM. c) XRD patterns of PDI powder (bottom) and PDI wires (top). Inset: the unit cell of PDI. d) Normalized UV-visible absorption and PL spectra. Dotted lines: PDI suspension in THF; solid lines: PDI wires deposited on quartz.

PL emission of PDI wires red-shifts by more than 100 nm and has enhanced 0–1 transition intensity at 691 nm and decreased 0–0 transition intensity at 640 nm. This change of relative intensity of the 0–0 and 0–1 transitions originates from the re-absorption of short wavelength PL emission.

In organic crystals, the molecular stacking as well as the direction of its optical transition dipole influences directly various optical properties such as refractive index, PL polarization state and nonlinear optical activity.[17] To clarify the optical anisotropy induced by the internal molecular orientation in the microwires, polarized optical microscopy was carried out, as shown in **Figure 2a**. Compared with the uniform PL intensity observed along the full length of the two crossed microwires in dark field, strong anisotropic PL emission was seen when the crossed microwires were placed between crossed polarizers (see Figure S3). This suggests that the PDI microwires are birefringent, which is usually observed in crystalline materials, flow-aligned glasses and polymers due to a preferred direction of internal molecular alignment.[17] In our case, the π-π stacking of PDI molecular along [100] direction leads to strong anisotropy of the refractive index and thus causes such birefringence.

Generally, the PL intensity is at its maximum when the emission polarizer is parallel to the dipole moment of the emissive molecule (i.e., long molecular axis) and it is at its minimum when the emission polarizer is perpendicular to the dipole moment of the emissive molecule.[18] For perylene and other elongated aromatic molecules in the polymer matrix, there is an angle of 27 ± 5° between the transition dipole moment and the orientation axis due to the specific interactions of the aromatic molecules with the polymer matrix.[16] Insight into the preferred direction of π-conjugate chain alignment in the PDI crystalline microwires can be obtained from polarization dependent PL spectroscopy of a single wire, as shown in Figure 2b and c. It is observed that the PL emission from the PDI microwire is polarization-dependent with a single axis of anisotropy. With the collection polarizer oriented an angle θ = 30° (also 210°) to the long axis of the wire, the highest PL intensities (I_{30}) are observed for the 0–0 and 0–1 peaks (at 639 and 688 nm). Conversely, at a polarized angle θ = 120° (also 300°), the PL intensities (I_{120}) of these two peaks are the lowest. An emission dichroic ratio, $R_d = I_{30}/I_{120}$, of 6.1 is obtained for the PL emission at 688 nm, corresponding to a polarization ratio ρ = 0.72, where $\rho = (R_d - 1)/(R_d + 1)$. This ratio is much larger than that of conjugated polymer nanowires (ρ = 0.6)[19] reported previously, and comparable to that of single-crystalline CdSe nanorods (ρ = 0.7–0.86).[20] Figure 2c shows the polar image of the PL peak intensities. The polarization-dependent behavior of the PDI wire PL is highly reproducible, and $\cos^2$ curves can be fitted to these data, which attests to the crystalline structure of the microwires and good alignment of the emissive molecules

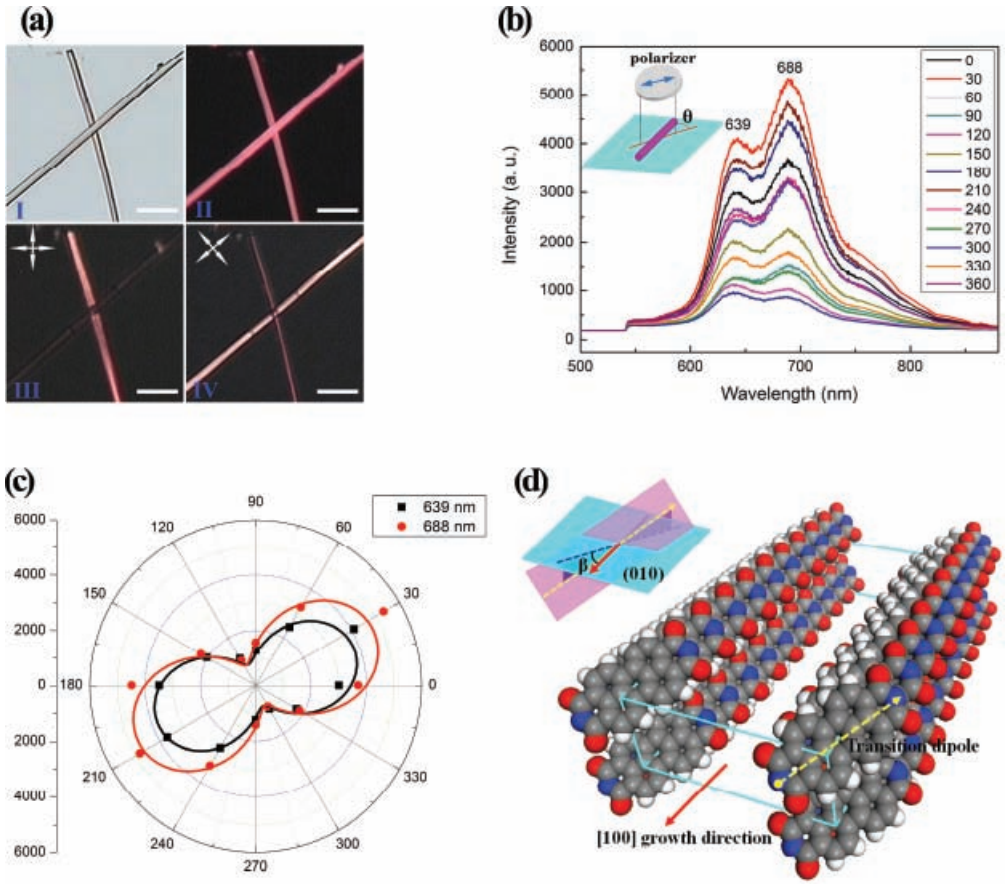

Figure 2. a) Polarized optical microscopy. I: bright-field optical image; II: dark field PL image; III and IV: polarized optical microscopy images. Scale bars: 20 μm. b) Polarized PL spectra obtained at variant angles (θ: 0~360°). Inset: θ refers to the relative angle between collection polarizer and the long axis of the PDI wire. c) Polar image of the peak intensities. Solid curves show $\cos^2$ fits. d) Schematic of 12 PDI units (the alkyl chains are not shown). Inset: β refers to the angle between the long axis and the projection of emission transition dipole in (010) plane.

along certain direction. At this point it is timely to recall the crystal structure of PDI wires resolved by XRD (Figure 1c), which is illustrated in the schematic of Figure 2d. It is clear that there is an angle of $\beta \approx 30°$ between the transition dipole moment and the preferential [100] growth direction, which is in good agreement with the experimental observation that the highest PL emission occurs at $\theta = 30°$ (Figures 2b, c).

Propagation loss measurements were carried out by looking at the spatially resolved PL spectra of the emitted light with respect to the distance travelled. Single-wire PL imaging and spectroscopy measurements were performed by local excitation of the wire, as shown schematically in **Figure 3a**. Figure 3b (bottom) shows a series of gray-color far-field PL microscopy images of a microwire (width: ~2.2 μm, length: ~150 μm). These pictures were captured by translating the excitation laser spot along the length of the wire. As a result, the propagation distance of waveguided PL prior to out-coupling at the rightmost tip increased gradually. It can be observed that the PL intensity at the right tip decreases with increasing propagation length. Figure 3c shows the intensity of the waveguided PL as a function of the propagation length. There are several notable features. Firstly, the out-coupled light intensity decreases exponentially as a function of increasing propagation distance, which is a typical characteristic of active waveguides. After normalizing the out-coupled PL intensity (I_{out}) with excitation PL intensity (I_{in}), I_{out}/I_{in} can be well-fitted by a first-order exponential decay function (inset of Figure 3c), expressed by $I_{out}/I_{in} = \exp(-\alpha x)$, where x is the propagation distance and α is a fitting parameter. This yielded a value of $\alpha = 302$ cm^{-1}, corresponding to a propagation loss of 0.13 dB μm^{-1}, which is much lower than PFO (poly(9,9-dioctyfluorene)) nanowires (0.48 dB μm^{-1})[2] and comparable to that of the recently reported organic crystalline microtubes (0.097 dB μm^{-1}).[5]

Secondly, we found that the out-coupled PL spectra exhibit relatively greater attenuation in the shorter wavelength region with increasing propagation distance compared to that of the 0–1 peak at longer wavelength. For example, the emissions below 640 nm are filtered almost completely by propagation of the light over a distance more than 40 μm. The normalized spectra in Figure 3d clearly reveal that there is overlap (yellow region) between UV absorption and PL emission, which will cause the re-absorption of the waveguided light during propagation of the PL. Consequently, the broad PL emission in the 600–800 nm region is narrowed and the full-width at half-maximum (FWHM) is reduced from 98 nm to 63 nm, as shown by the upper inset of Figure 3d. The 0–1 emission peak

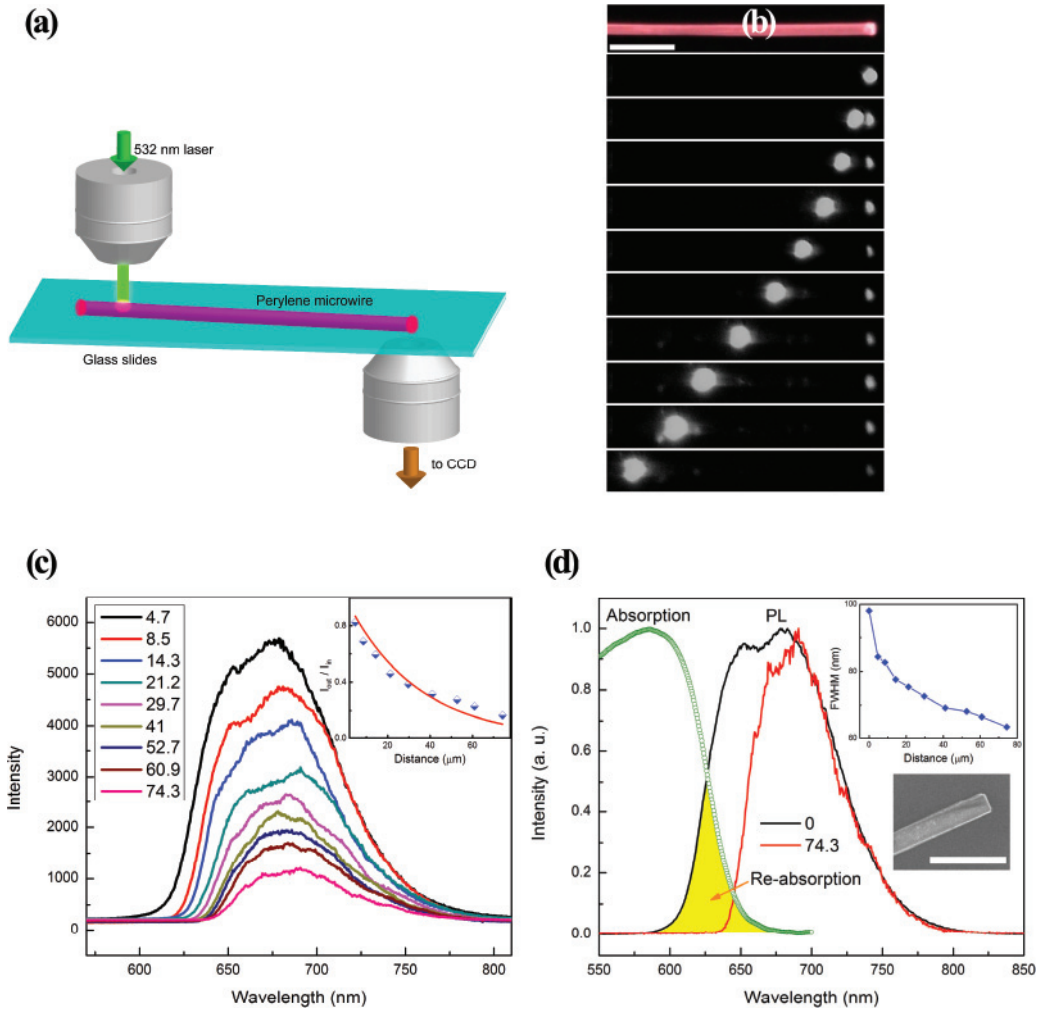

Figure 3. a) Schematic of the waveguide measurement. b) Top: dark field optical image, scale bar: 20 μm. Bottom: PL images showing optical waveguide upon laser excitation at different positions. c) Spatially resolved PL spectra of waveguide emission out-coupled at the tip of the microrwire shown in (b). Inset shows I_{out}/I_{in} versus propagation distance and exponential fit (red line). d) Normalized out-coupled PL spectra at propagation distance of 0 and 74.3 μm. UV-visible absorption spectrum is also normalized for reference. Upper inset: FWHM of out-coupled PL spectra versus propagation distance. Lower inset: scanning electron microscopy (SEM) image of wire end, scale bar: 10 μm.

is slightly red-shifted about 10 nm after the waveguide light propagates 74.3 μm. Thus, the short wavelength light is modulated upon routing through the PDI microwire.

It is noteworthy that resonances or modes were observed superimposed upon the 0–1 peak of the out-coupled spectrum (red curve in Figure 3d), which can be assigned to axial Fabry-Pérot type cavity resonances.[1,2,21] This type of cavity behavior could be especially prominent for nano/micro wire waveguides incorporating planar, reflective end facets that are capable of providing the requisite cavity feedback. Due to the cleaved end face of the measured wire (lower inset of Figure 3d), longitudinal micro-cavity effects could be operational within the PDI wires. Based on a simple estimation proposed by Balzer et al.,[22,23] we conclude that the PDI wires have potential to act as multi-mode waveguides (See Supporting Information, Figure S4).

The intensity modulation in semiconductor electro-optic modulators is achieved by the local electric field induced modulation of the absorption coefficient or refractive index.[24,25] Electro-optical modulators were fabricated on the PDI microwires to explore the electrical field modulation on optical waveguide based on a parallel-plate capacitor structure, as shown schematically in **Figure 4a**. A typical device is shown in Figure 4b, in which the PDI microwire is electrically insulated from the top and back electrodes by silicon oxide and poly(methyl methacrylate) (PMMA), respectively. A significant decrease of the out-coupled PL intensity at the end of the microwire was observed with increasing bias voltage, as illustrated in Figure 4c and d. This intensity modulation is reversible when the bias voltage is swept between 0 and 30 V. The intensity modulation scales linearly as a function of the applied voltage up to 15 V, as shown by the plot in Figure 4e, and deviates slightly from linearity at larger voltages; an attenuation of –1.3 dB is achieved at 30 V. The local electric field distribution within the device was simulated by finite element method (See supporting information, Figure S5), as shown in Figure 4f. A field strength of ~2.01×10^5 V cm^{-1} in PDI wire is generated

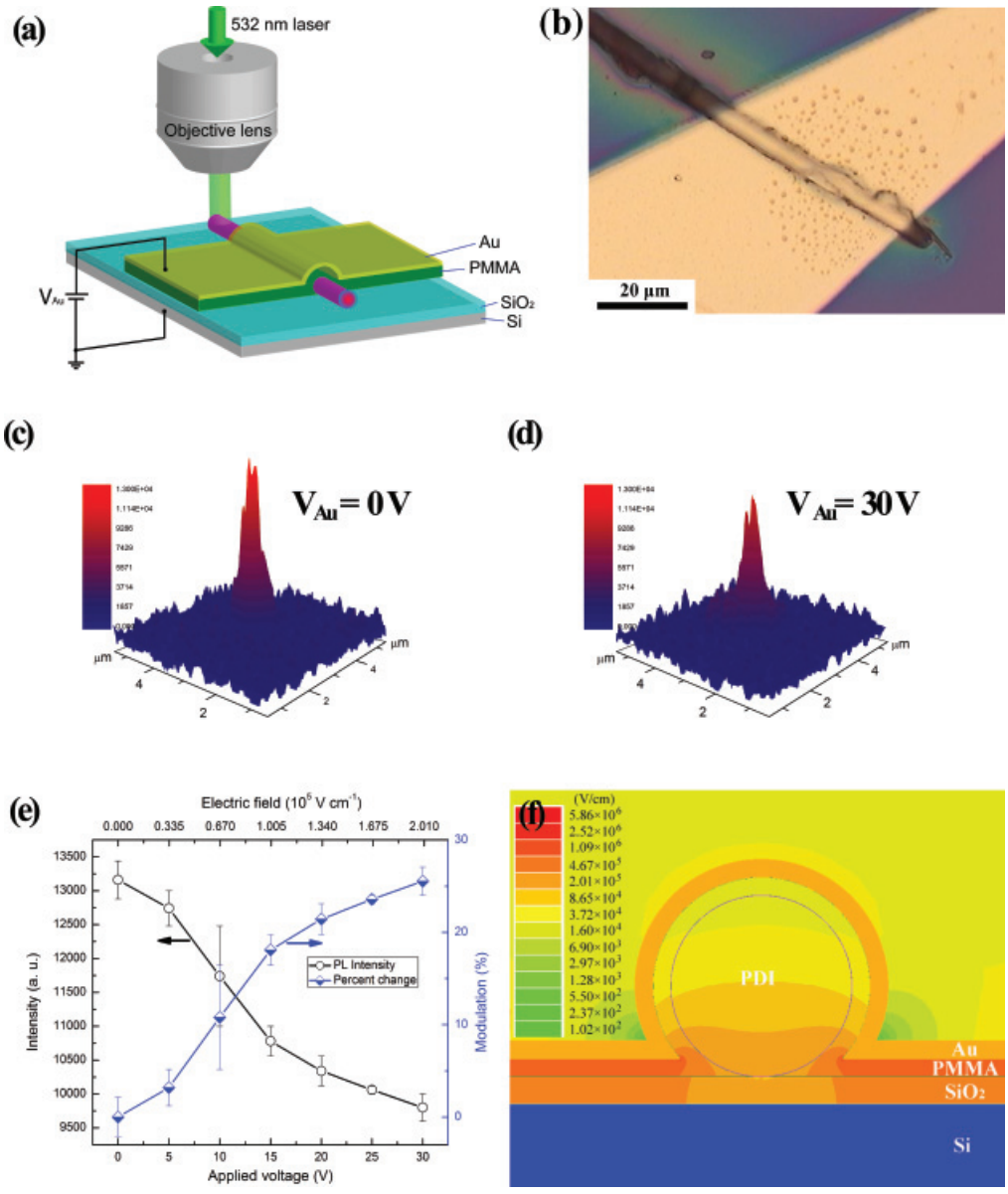

Figure 4. Electrical modulation of waveguiding in PDI microwire. a) Schematic and b) optical image of the electrical-optical modulator. c, d) Out-coupled PL intensity. c): V_{Au} = 0 V; d): V_{Au} = 30 V. e) PL Intensity modulation versus applied voltage V_{Au}. f) Simulated electrical field distribution in the cross-section of the device (V_{Au} = 30 V).

while applying a bias voltage of 30 V, as a result, a modulation of 26% is obtained, which is comparable to that of CdS nanowire modulator[24] under similar electric field strength.

In summary, we report the first optical waveguide based on PDI crystalline microwires. PDI is a good polymeric electro-optic material because of its low relative permittivity, low operating voltage, high thermal and photo-stability, and easy integration on flexible substrates. The tilted stacking of the π-conjugated perylene molecules gives rise to an angle between the transition dipole moment and the microwire axis. This internal molecular alignment results in the anisotropy of refractive index and produces strong birefringence and polarized PL emission. The highly crystalline structure as well as smooth wire surface results in high PL efficiency and low propagation loss. We demonstrate electrically modulated waveguide in PDI wires with a modulation of 26%. The basic optoelectronic functions demonstrated in this work reveal the good potential of perylene crystalline wires to function as polarizer, waveguide and modulator and pave the way for flexible electro-optic modulators based on organic materials.

Experimental Section

For the synthesis of PDI microwires, PDI (Sigma Aldrich) was added into GO solution (1 mg mL^{-1}, made by a modified Hummers method[26,27])

with a GO to PDI mass ratio of 1:2. The mixture was then refluxed at ~80 °C for 24 h. After that, the composite was washed with DMF:ethanol (1:5) by centrifuging at 11500 rpm until the colorless supernatant was obtained to ensure that all the unreacted PDI is removed. The resulting GO-PDI composite was dried in vacuum, following by dissolving in DMF (0.5 mg mL^{-1}). The solution was then subjected to a hydrothermal process at ~180 °C for 24 h to produce PDI wires. The synthesized composites were filtrated and washed with DMF. All the synthesized materials were kept in vacuum desiccators.

TEM measurements were conducted with a JEOL TEM-3010 microscope (acceleration voltage: 300 kV). The crystal structure of PDI wires was investigated using 8.048 keV photons (CuKα1 radiation equivalent) radiation source selected by a Si (111) channel-cut monochromator. The UV-visbile absorption and PL spectra were measured on Shimadzu UV2450 UV-Vis spectrophotometer and Perkin Elmer LS55 luminescence spectrometer, respectively. PDI wire suspension was spin-coated onto a cover glass substrate (thickness: 0.17 mm) to achieve random orientation and distribution of these wires for further optical studies. Optical polarization microscopy was performed on an Olympus BX 51 microscope with two crossed polarizers (see Figure S3 in the Supporting Information). The polarized PL spectra, waveguide characteristics and the electro-optical modulations of individual PDI microwire were carried out with a WITEC CRM 200 confocal Raman system, as described in our previous work.[8] The sample for electro-optical modulation was prepared by the following procedure: PDI microwire suspension was drop-casted on SiO_2 (thickness: 285 nm)/Si substrate, then ~200 nm thick PMMA was spin-coated on the sample substrate and baked at 120 °C for 15 min, followed by thermal evaporation of Au thin-film electrodes (thickness: ~200 nm) using parallel copper grids as shadow mask. All measurements were performed at room temperature.

Supporting Information

Supporting Information is available online from Wiley InterScience or from the author.

Acknowledgements

The authors thank MOE grant "Structure and Dynamics of Molecular Self-Assembled Layers" R-143–000-344–112.

Received: February 26, 2010
Published online: July 7, 2010

[1] D. O'Carroll, I. Lieberwirth, G. Redmond, *Nature Nanotech.* **2007**, *2*, 180.
[2] D. O'Carroll, I. Lieberwirth, G. Redmond, *Small* **2007**, *3*, 1178.
[3] K. Takazawa, Y. Kitahama, Y. Kimura, G. Kido, *Nano Lett* **2005**, *5*, 1293.
[4] Y. S. Zhao, A. Peng, H. Fu, Y. Ma, J. Yao, *Adv. Mater.* **2008**, *20*, 1661.
[5] Q. Liao, H. Fu, J. Yao, *Adv. Mater.* **2009**, *21*, 4153.
[6] M. Law, D. J. Sirbuly, J. C. Johnson, J. Goldberger, R. J. Saykally, P. Yang, *Science* **2004**, *305*, 1269.
[7] D. J. Sirbuly, M. Law, H. Yan, P. Yang, *J. Phys. Chem. B* **2005**, *109*, 15190.
[8] B. Yan, L. Liao, Y. M. You, X. J. Xu, Z. Zheng, Z. X. Shen, J. Ma, L. M. Tong, T. Yu, *Adv. Mater.* **2009**, *21*, 2436.
[9] F. Würthner, *Chem. Commun.* **2004**, *2004*, 1564.
[10] P. Peumans, S. Uchida, S. R. Forrest, *Nature* **2003**, *425*, 158.
[11] A. L. Briseno, S. C. B. Mannsfeld, C. Reese, J. M. Hancock, Y. Xiong, S. A. Jenekhe, Z. Bao, Y. Xia, *Nano Lett.* **2007**, *7*, 2847.
[12] H. Liu, Y. Li, S. Xiao, H. Gan, T. Jiu, H. Li, L. Jiang, D. Zhu, D. Yu, B. Xiang, Y. Chen, *J. Am. Chem. Soc.* **2003**, *125*, 10794.
[13] K. Balakrishnan, A. Datar, T. Naddo, J. Huang, R. Oitker, M. Yen, J. Zhao, L. Zang, *J. Am. Chem. Soc* **2006**, *128*, 7390.
[14] K. Balakrishnan, A. Datar, R. Oitker, H. Chen, J. Zuo, L. Zang, *J. Am. Chem. Soc.* **2005**, *127*, 10496.
[15] L. Zang, Y. Che, J. S. Moore, *Acc. Chem. Res.* **2008**, *41*, 1596.
[16] C. W. Struijk, A. B. Sieval, J. E. J. Dakhorst, M. van Dijk, P. Kimkes, R. B. M. Koehorst, H. Donker, T. J. Schaafsma, S. J. Picken, A. M. van de Craats, J. M. Warman, H. Zuilhof, E. J. R. Sudholter, *J. Am. Chem. Soc.* **2000**, *122*, 11057.
[17] D. O'Carroll, G. Redmond, *Chem. Mater.* **2008**, *20*, 6501.
[18] F. Balzer, H. G. Rubahn, *Adv. Funct. Mater.* **2005**, *15*, 17.
[19] S. Moynihan, P. Lovera, D. O'Carroll, D. Iacopino, G. Redmond, *Adv. Mater.* **2008**, *20*, 2497.
[20] J. Hu, L.-s. Li, W. Yang, L. Manna, L.-w. Wang, A. P. Alivisatos, *Science* **2001**, *292*, 2060.
[21] J. C. Johnson, H. Yan, P. Yang, R. J. Saykally, *J. Phys. Chem. B* **2003**, *107*, 8816.
[22] F. Balzer, V. G. Bordo, A. C. Simonsen, H. G. Rubahn, *Phys. Rev. B* **2003**, *67*, 115408.
[23] F. Balzer, V. G. Bordo, A. C. Simonsen, H. G. Rubahn, *Appl. Phys. Lett.* **2003**, *82*, 10.
[24] C. J. Barrelet, A. B. Greytak, C. M. Lieber, *Nano Lett.* **2004**, *4*, 1981.
[25] A. B. Greytak, C. J. Barrelet, Y. Li, C. M. Lieber, *Appl. Phys. Lett.* **2005**, *87*, 151103.
[26] K. P. Loh, Q. L. Bao, P. K. Ang, J. X. Yang, *J. Mater. Chem.* **2010**, *20*, 2277.
[27] Y. Zhou, Q. L. Bao, L. A. L. Tang, Y. L. Zhong, K. P. Loh, *Chem. Mater.* **2009**, *21*, 2950.